ResearchGate

See discussions, stats, and author profiles for this publication at: https://www.researchgate.net/publication/8444438

Elastic Properties of Single Amylose Chains in Water: A Quantum Mechanical and AFM Study

ARTICLE *in* JOURNAL OF THE AMERICAN CHEMICAL SOCIETY · AUGUST 2004

Impact Factor: 12.11 · DOI: 10.1021/ja031940x · Source: PubMed

CITATIONS
35

READS
39

5 AUTHORS, INCLUDING:

Wiesław Nowak
Nicolaus Copernicus University
84 PUBLICATIONS **703** CITATIONS
SEE PROFILE

Gwangrog Lee
Gwangju Institute of Science and Technology
20 PUBLICATIONS **521** CITATIONS
SEE PROFILE

Piotr E Marszalek
Duke University
78 PUBLICATIONS **2,940** CITATIONS
SEE PROFILE

Available from: Piotr E Marszalek
Retrieved on: 26 January 2016

J|A|C|S
ARTICLES
Published on Web 07/03/2004

Elastic Properties of Single Amylose Chains in Water: A Quantum Mechanical and AFM Study

Zhenyu Lu,[†] Wieslaw Nowak,[‡,§] Gwangrog Lee,[‡] Piotr E. Marszalek,*[,‡] and Weitao Yang*[,†]

Contribution from the Department of Chemistry, Duke University, Durham, North Carolina 27708, Department of Mechanical Engineering and Materials Science, CBIMMS, Durham, North Carolina 27708, and Institute of Physics, Nicholas Copernicus University, 87-100 Torun, Poland

Received December 24, 2003; E-mail: pemar@duke.edu; weitao.yang@duke.edu

Abstract: Recent single-molecule atomic force microscopy (AFM) experiments have revealed that some polysaccharides display large deviations from force−extension relationships of other polymers which typically behave as simple entropic springs. However, the mechanism of these deviations has not been fully elucidated. Here we report the use of novel quantum mechanical methodologies, the divide-and-conquer linear scaling approach and the self-consistent charge density functional-based tight binding (SCC-DFTB) method, to unravel the mechanism of the extensibility of the polysaccharide amylose, which in water displays particularly large deviations from the simple entropic elasticity. We studied the deformations of maltose, a building block of amylose, both in a vacuum and in solution. To simulate the deformations in solution, the TIP3P molecular mechanical model is used to model the solvent water, and the SCC-DFTB method is used to model the solute. The interactions between the solute and water are treated by the combined quantum mechanical and molecular mechanical approach. We find that water significantly affects the mechanical properties of maltose. Furthermore, we performed two nanosecond-scale steered molecular dynamics simulations for single amylose chains composed of 10 glucopyranose rings in solution. Our SCC-DFTB/MM simulations reproduce the experimentally measured force−extension curve, and we find that the force-induced chair-to-boat transitions of glucopyranose rings are responsible for the characteristic plateau in the force−extension curve of amylose. In addition, we performed single-molecule AFM measurements on carboxymethyl amylose, and we found that, in contrast to the results of an earlier work by others, these side groups do not significantly affect amylose elasticity. By combining our experimental and modeling results, we conclude that the nonentropic elastic behavior of amylose is governed by the mechanics of pyranose rings themselves and their force-induced conformational transitions.

Introduction

Pyranose ring-based sugars and polysaccharides are ubiquitous and play fundamental roles in biological systems by providing energy, serving as structural elements, and participating in cellular recognition, signaling, and adhesive events. While serving as structural elements or when engaged in intermolecular interactions, sugar rings are frequently placed under mechanical stress. However, little is known about how sugar rings respond to these stresses. On the basis of recent measurements of the elasticity of individual polysaccharide chains using atomic force microscopy (AFM), it has been suggested that stressed sugar rings may be significantly deformed by mechanical forces which can twist and bend their bond angles.[1] Other AFM studies have suggested that sugar rings in a stretched polysaccharide chain can even switch their preferred chair conformation to a boat[2,3] or an inverted chair conformation,[4−6] both of which are more extended and higher in energy. These ideas of force-induced conformational transitions attempt to explain the large deviations from the simple entropic elasticity of polymers[7,8] that are prominently displayed by α-linked polysaccharides, such as amylose, dextran, and pectin.[1−6,9−11] Such conformational transitions are thought to be promoted by axial bonds of α-linked

[†] Duke University.
[‡] CBIMMS.
[§] Nicholas Copernicus University.

(1) Rief, M.; Oesterhelt, F.; Heymann, B.; Gaub, H. E. *Science* **1997**, *275*, 1295−1297.
(2) Marszalek, P. E.; Oberhauser, A. F.; Pang, Y.-P.; Fernandez, J. M. *Nature* **1998**, *396*, 661−664.
(3) Marszalek, P. E.; Li, H.; Oberhauser, A. F.; Fernandez, J. M. *Proc. Natl. Acad. Sci. U.S.A.* **2002**, *99*, 4278−4283.
(4) Marszalek, P. E.; Pang, Y.-P.; Li, H.; El Yazal, J.; Oberhauser, A. F.; Fernandez, J. M. *Proc. Natl. Acad. Sci. U.S.A.* **1999**, *96*, 7894−7898.
(5) Marszalek, P. E.; Li, H.; Fernandez, J. M. *Nature Biotechnol.* **2001**, *19*, 258−262.
(6) Marszalek, P. E.; Oberhauser, A. F.; Li, H.; Fernandez, J. M. *Biophys. J.* **2003**, *85*, 2696−2704.
(7) Flory, P. J. *Principles of Polymer Chemistry*; Cornell University Press: Ithaca, 1953.
(8) Flory, P. J. *Statistical Mechanics of Chain Molecules*; Hanser Publishers: München, Germany,1988.
(9) Li, H. B.; Rief, M.; Oesterhelt, F.; Zhang, X.; Shen, J. C.; Gaub, H. E. *Chem. Phys. Lett.* **1999**, *305*, 197−201.
(10) Grandbois, M.; Beyer, M.; Rief, M.; Clausen-Schaumann, H.; Gaub, H. E. *Science* **1999**, *283*, 1727−1730.
(11) Brant, D. A. *Curr. Opin. Struct. Biol.* **1999**, *9*, 556−562.

polysaccharides, which, working as atomic levers, produce the necessary torque to trigger conformational transitions in the ring.[4]

From the aspect of computational modeling, the elastic properties of polysaccharides have been rarely addressed. However, the structures and energetics of pyranose rings have been well studied, providing valuable information for the current work. Early studies[12,13] demonstrated that the polymorphic transformations of amylose may correlate significantly with monomeric geometry changes. In subsequent studies, molecular mechanics force field calculations were performed to investigate the flexibility of monomeric pyranose rings. Pensak and French[14] showed that, in the chair form, α-D-glucopyranose can be deformed easily, resulting in a range of O4−O1 distances. Further works[15,16] constructed conformational energy maps using the ring puckering parameters and described the energetics of the pyranose rings in a full range of shapes. In addition to the force field studies, ab initio quantum mechanical calculations were also performed for the deformation of a single glucose ring.[17] The above calculations are useful in that they provide information about possible conformational pathways and final deformed conformations of monomeric pyranose rings. However, to our knowledge, there is only one study that modeled the deformation of a polysaccharide chain. This work, which provides atomistic details of the polymer during the stretching process, was done by Heymann and Grubmüller.[18] They investigated the origin of a large deviation of amylose elasticity from the freely jointed chain model of entropic elasticity.[7] This large deviation manifests itself as a large plateau starting at a force of ∼250 pN in the force−extension relationship. They performed force field simulations of amylose chains in a vacuum. Upon the application of a stretching force, they observed frequent chair-to-boat transitions of the glucopyranose rings, but the force−extension relationship obtained from the MD simulations failed to reproduce the characteristic plateau feature. The plateau became pronounced only after they chose a two-fold screw axis conformation for the amylose chain and added a significant restraint on the inter-monomeric rotational motion. These authors assumed that the necessary restraint represented the limitation imposed on the intra-monomer mobility by bulky or charged side groups that were present on amylose used in the AFM experiments. In addition, they proposed that, by introducing or removing such bulky or charged substituents on the glucopyranose ring, one could tailor the elastic properties of this polysaccharide. However, these ideas have never been tested experimentally or supported by ab initio quantum mechanical calculations, the latter being computationally unfeasible for large systems. In addition, ab initio quantum mechanical calculations are typically done in a vacuum, and they tend to generate strong intramolecular hydrogen bonds in sugar rings. Thus, the resulting conformations may not be representative of those in water,[20] where AFM stretching experiments are carried out.

To investigate the effect of the ring substituents, we performed AFM stretching measurements on single molecules of carboxymethylated amylose (CMA). The results show that the side-group substituents have little effect on the elastic properties of amylose, an observation that does not support the conclusion from the previous work mentioned above. To clarify this ambiguity, we performed our own modeling work. We used the recently developed self-consistent charge density functional-based tight binding (SCC-DFTB) method[21] combined with the divide-and-conquer (DAC) linear scaling approach[22−26] for electronic structure calculations. First we studied the deformation of maltose by carrying out constrained minimizations over a wide range of O4′−O1 distances and compared the energy profiles of ab initio density functional theory (DFT) and SCC-DFTB calculations. Subsequently, we stretched the maltose molecule both in a vacuum and in solution with the steered molecular dynamics (SMD) approach.[27] We studied the influences of solvent on the shape of force−extension curves and found that the solvent is important to the mechanical properties of maltose. Finally, we modeled the stretching of amylose chains in solution and obtained force−extension curves comparable to the AFM data. Our results show that the plateau region in the force−extension relationship of amylose is indeed related to the chair−boat transition of pyranose rings, supporting the earlier conjecture from AFM experiments. Note that, for all the simulations performed in solution, the TIP3P molecular mechanical model[28] is used to model the solvent water, and the SCC-DFTB method is used to model the solute (maltose or amylose chains). The interactions between the solute and the water are treated by the combined quantum mechanical and molecular mechanical (QM/MM) approach.

Our current theoretical approach provides an alternative way to model large biological polymers in water, allows us to gain insight into the structure−elasticity relationship at an atomic level, and helps us to interpret the results of single-molecule AFM measurements. This in turn will help us to further develop single-molecule force spectroscopy as a useful methodology in carbohydrate and biophysical research.

We note that, within the whole context, for simplicity, we use the O1−C1−C2−O2 angle to characterize the chair-to-boat transition, and we routinely call a conformation "boat" even though the structure may actually appear to be a "skew". To make the current work comparable with others, in the Supporting Information we report the results for maltose using the Cremer−Pople ring-pucking parameters,[29] which are standard in describing conformations of the sugar rings.

(12) French, A. D.; Murphy, V. G. *Carbohydr. Res.* **1973**, *27*, 391−406.
(13) French, A. D.; Murphy, V. G. *Polymer* **1977**, *18*, 489−494.
(14) Pensak, D. A.; French, A. D. *Carbohydr. Res.* **1980**, *87*, 1−10.
(15) Joshi, N. V.; Rao, V. S. *Biopolymers* **1979**, *18*, 2993−3004.
(16) Dowd, M. K.; French, A. D.; Reilly, P. J. *Carbohydr. Res.* **1994**, *264*, 1−19.
(17) O'Donoghue, P.; Luthey-Schulten, Z. A. *J. Phys. Chem. B* **2000**, *104*, 10398−10405.
(18) Heymann, B.; Grubmüller, H. *Chem. Phys. Lett.* **1999**, *305*, 202−208.
(19) Gessler, K.; Usón, I.; Takaha, T.; Kraus, N.; Smith, S. M.; Okada, S.; Sheldrick, G. M.; Saenger, W. *Proc. Natl. Acad. Sci. U.S.A.* **1999**, *96*, 4246−4251.
(20) Kirschner, K. N.; Woods, R. J. *Proc. Natl. Acad. Sci. U.S.A.* **2001**, *98*, 10541−10545.
(21) Elstner, M.; Porezag, D.; Jungnickel, G.; Elsner, J.; Haugk, M.; Frauenheim, Th.; Suhai, S. *Phys. Rev. B* **1998**, *58*, 7260−7268.
(22) Yang, W. *Phys. Rev. Lett.* **1991**, *66*, 1438−1441.
(23) Yang, W.; Lee, T.-S. *J. Chem. Phys.* **1995**, *103*, 5674−5678.
(24) Lee, T.-S.; York, D.; Yang, W. *J. Chem. Phys.* **1996**, *105*, 2744−2750.
(25) Lewis, J. P.; Carter, C. W., Jr.; Hermans, J.; Pan, W.; Lee, T.-S.; Yang, W. *J. Am. Chem. Soc.* **1998**, *120*, 5407−5410.
(26) Liu, H.; Elstner, M.; Kaxiras, E.; Frauheim, Th.; Hermans, J.; Yang, W. *Proteins: Stuct., Funct. Genet.* **2001**, *44*, 484−489.
(27) Isralewitz, B.; Gao, M.; Schulten, K. *Curr. Opin. Struct. Biol.* **2001**, *11*, 224−230.
(28) Jorgensen, W. L.; Chandrasekhar, J.; Madura, J.; Impey, R. W.; Klein, M. L. *J. Chem. Phys.* **1983**, *79*, 926−933.
(29) Cremer, D.; Pople, J. A. *J. Am. Chem. Soc.* **1975**, *97*, 1354−1358.

Computational and Experimental Methods

Single-Molecule AFM Measurements on Carboxymethylamylose (CMA). Amylose was derivatized to CMA sodium salt by Carbomer, Inc. (San Diego, CA). The degree of substitution (DS) was verified by NMR to be greater than 1 (Carbomer, Inc.). CMA sodium salt was dissolved in phosphate-buffered saline (PBS) buffer at a concentration of 0.01−0.05% (w/v), and a layer of polysaccharide was created by drying a drop of this solution onto a glass coverslip, followed by extensive rinsing with 18 MΩ water. After drying, samples were rehydrated in PBS solution for AFM measurements. Our setups consist of a PicoForce AFM from Veeco Instruments, Inc./Digital Instruments (Santa Barbara, CA) and a homemade single-axis instrument similar to that described in earlier publications.[30] The spring constant of each individual AFM cantilever was calibrated using the thermal noise method described by Florin et al.[31]

Divide-and-Conquer (DAC) Linear-Scaling Self-Consistent Charge Density Functional-Based Tight Binding and Molecular Mechanical Combined (SCC-DFTB/MM) Approach. To model the deformation of a polysaccharide chain in solution, the SCC-DFTB quantum mechanical method and the TIP3P molecular mechanics model[28] were used for the solute and the solvent, respectively. This SCC-DFTB and molecular mechanical combined (SCC-DFTB/MM) approach has been applied successfully to the simulations of small peptides[32] and proteins.[26,33] In this approach, the total Hamiltonian of the system is given by

$$H_{\text{total}} = H_{\text{QM}} + H_{\text{MM}} + H_{\text{QM/MM}} \tag{1}$$

where the interaction Hamiltonian, $H_{\text{QM/MM}}$, is comprised of two terms, $H^{\text{ele}}_{\text{QM/MM}}$ and $E^{\text{vdW}}_{\text{QM/MM}}$. These two terms describe the Coulomb and van der Waals interactions between the solute and the solvent. Consistent with the treatment of Coulomb interactions in SCC-DFTB, $H^{\text{ele}}_{\text{QM/MM}}$ is given by

$$H_{\mu\nu} = -\frac{1}{2}S_{\mu\nu}\sum_{\beta\in\text{MM}}\left(\frac{1}{R_{\mu\beta}} + \frac{1}{R_{\nu\beta}}\right)Q_\beta \tag{2}$$

where $S_{\mu\nu}$ is the overlap matrix element, $R_{\mu\beta}$ is the distance between the corresponding QM and MM atoms, and Q_β is the MM point charge. The corresponding QM/MM electrostatic interaction energy is

$$E^{\text{ele}}_{\text{QM/MM}} = -\sum_{\alpha\in\text{QM}}\sum_{\beta\in\text{MM}}\frac{\Delta q_\alpha Q_\beta}{R_{\alpha\beta}} \tag{3}$$

which takes the same form of the classical Coulomb interactions used in conventional force fields. For the QM/MM van der Waals interactions, the pairwise atomic Lennard-Jones potential is used. The long-range van der Waals interaction, which is absent in density functional theory-based calculations, is explicitly included with the form $-f_{\text{d}}(R)C_6/R^6$, where C_6/R^6 is the attractive term of the Lennard-Jones potential and f_{d} is the damping function to switch off this interaction at short distances.[26,34] All the van der Waals parameters were taken from the Amber95 force field.[35] The divide-and-conquer (DAC) linear-scaling approach[22,23] was used to diagonalize the SCC-DFTB Hamiltonian. The polysaccharide chain was divided into 10 subsystems. Each subsystem consisted of a glucose ring, and the cutoff of the buffer region was 5.0 Å. The DAC linear-scaling SCC-DFTB/MM method was implemented by Liu et al.,[26] and the TINKER program package[36] was used for all force field calculations and molecular dynamics simulations.

Steered Molecular Dynamics Simulations. The AFM experiment was simulated with the steered molecular dynamics (SMD) method,[27] which examines the behavior of molecules when they are driven out of their equilibrium conformations by external forces. The O4 atom of the first sugar ring (the nonreducing end) was restrained to a fixed position using a harmonic potential with a force constant of 100 kcal mol^{-1} Å^{-2}. The O1 atom of the last sugar ring (the reducing end) was subjected to a time-dependent spring force,

$$F_{\text{spring}} = k_{\text{cant}}[z_{\text{cant}}(t) - z_{\text{O1}}(t)] \tag{4}$$

where z_{cant} and z_{O1} are the coordinates (projected on the pulling direction) of the cantilever and the O1 atom of the last sugar ring. The cantilever moved with a constant velocity υ_{cant}. For the simulations of pulling the polysaccharide chains, the spring force constant k_{cant} and the cantilever velocity υ_{cant} were chosen to be 1.0 kcal mol^{-1} Å^{-2} and 0.05 Å ps^{-1}, respectively. For the stretching of maltose, υ_{cant} was chosen to be 0.1 Å ps^{-1}. The time step used in the simulations was 1 fs, and all bonds involving hydrogen atoms were constrained using the rattle algorithm.[37] The temperature was controlled using the weak coupling method.[38] For the simulations in solution, the nonbonded interactions were calculated with a 12.0 Å cutoff distance, and the nonbonded pairlist was updated every 10 time steps with a 13.5 Å cutoff distance.

Maltose Stretching. The computer model of maltose was generated with the program Spartan V02 for Windows. The two residues were arranged in an antiparallel configuration with the Ψ angle close to 60° (the torsion angles for maltose are defined as Φ = O5′−C1′−O4−C4 and Ψ = C1′−O4−C4−C5). The C6′−O6′ group was positioned to be in the gg orientation, while the C6−O6 group was in the gt orientation. All hydroxyl groups were placed in a clockwise orientation. The structure was then minimized at the B3LYP/6-31+G(d) level. The potential energy surface (PES) scan was carried out by constraining the O4′−O1 distances and optimizing the remaining degrees of freedom at the B3LYP/6-311++G(d,p) level. The ab initio DFT calculations were performed using the PQS program.[39] To test our method, the SCC-DFTB Hamiltonian was used to calculate the energy profile for the set of geometries optimized from the above B3LYP PES scan.

We performed a 400 ps SMD simulation in a vacuum and 200 ps in solution at a constant temperature of 300 K. The coupling time used for temperature control was chosen to be 0.05 ps. For the solution simulation, the solute and solvent were coupled to external baths separately.

Stretching Amylose Chains. Because the structure of amylose in solution remains unclear, two different conformations of the amylose fragment (10 glucose rings, 213 atoms) were constructed. One amylose fragment took a two-fold screw axis conformation (see Figure 2B, top), as suggested by Heymann and Grubmüller.[18] However, in contrast to ref 18, we did not apply any restraints on the inter-monomeric rotational flexibility of the sugar rings for a reason to be explained later. Another amylose fragment took a randomized orientation for neighboring monomers. The constructed amylose fragments were then solvated with a pre-equilibrated TIP3P water box of dimensions 30 Å × 30 Å × 80 Å. The entire systems were minimized until the energy gradient was less than 1 kcal mol^{-1} Å^{-1} and equilibrated for 50 ps at 300 K before the external forces were added. The Ψ and Φ values of the initial

(30) Oberhauser, A. F.; Marszalek, P. E.; Erickson, H. P.; Fernandez, J. M. *Nature* **1998**, *393*, 181−185.
(31) Florin, E. L.; Rief, M.; Lehmann, H.; Ludwig, M.; Dornmair, C.; Moy, V. T.; Gaub, H. E. *Biosens. Biolelectron.* **1995**, *10*, 895−901.
(32) Hu, H.; Elstner, M.; Hermans, J. *Proteins: Stuct., Funct. Genet.* **2003**, *50*, 451−463.
(33) Cui, Q.; Elstner, M.; Kaxiras, E.; Frauenheim, T.; Karplus, M. *J. Phys. Chem. B* **2001**, *105*, 569−585.
(34) Elstner, M.; Frauenheim, T.; Suhai, S. *J. Mol. Struct. (THEOCHEM)* **2003**, *632*, 29−41.
(35) Cornell, W. D.; Cieplak, P.; Bayly, C. I.; Gould, I. R.; Merz, K. M.; Ferguson, D. M.; Spellmeyer, D. C.; Fox, T.; Caldwell, J. W.; Kollman, P. A. *J. Am. Chem. Soc.* **1995**, *117*, 5179−5197.
(36) Ponder, J. W. *TINKER, Software Tools for Molecular Design, Version 3.6*; the most updated version of the TINKER program can be obtained from J. W. Ponder's World Wide Web site at http://dasher.wustl.edu/tinker (February 1998).
(37) Andersen, H. C. *J. Comput. Phys.* **1983**, *52*, 24−34.
(38) van Gunsteren, W. F.; Berendsen, H. J. C.; Colonna, F.; Perahia, D.; Hollenberg, J. P.; Lellouch, D. *J. Comput. Chem.* **1984**, *5*, 272−279.
(39) The pqs ab initio program package version 2.4; Web site http://www.pqs-chem.com.

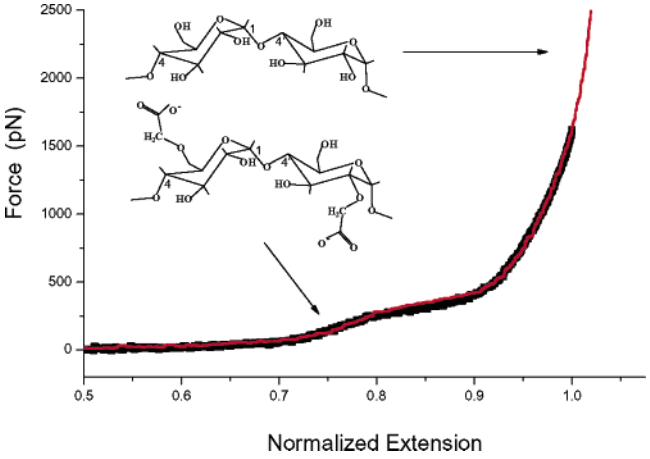

Figure 1. Comparison of force spectrograms of amylose and its carboxymethyl derivative (CMA). The elasticity of CMA (black curve) (degree of substitution, DS > 1) is indistinguishable from that of pure amylose (red line). The characteristic plateau feature in CMA starts at a force of 263 ± 49 pN (averaged over 6 measurements), as compared to 275 ± 45 pN (averaged over 11 measurements) for amylose. The inset shows the structure of amylose and CMA. The putative substitution sites in CMA are depicted at positions 2 and 6. AFM experiments on amylose were carried out in water[2] and on CMA in PBS solution (this study). The traces shown represent two individual recordings obtained on single molecules and not averages of several recordings.

conformations are shown in Table 2. Two 900 ps steered molecular dynamics simulations were performed for the two-fold screw axis and randomized amylose fragments.

All the results are presented with the data collected every 1 ps. To compare with experimental results, the length of the polysaccharide chains is normalized with 55.3 Å, which is the average length determined at the force of 2000 pN.

Results and Discussion

AFM Experiment on CMA. Because commercially available CMA used in earlier AFM studies[3,9] has an unknown degree of substitution (most likely much less than 1), we decided to derivatize amylose ourselves and introduce at least one carboxymethyl group per glucopyranose ring. The results obtained on single CMA molecules are presented in Figure 1, which also compares the force spectrogram of CMA to that of underivatized amylose.[2,3] We find that the force spectrograms of CMA and amylose are indistinguishable, which suggests that the carboxymethyl groups, at the level of one per glucose ring and at a high salt concentration (PBS buffer), do not affect the elasticity of amylose. This result does not support the conclusion from the recently published molecular dynamics simulations of amylose that bulky substituents should significantly affect its elasticity by restricting the inter-monomeric rotational flexibility of the pyranose rings.[18]

Additional information can be obtained from this experiment. It is well known that amylose chains have a tendency to form helical turns in solution while maintaining the overall configuration of a random coil.[40,41] The presence of these secondary structure elements has been demonstrated with a simple iodine test that turns amylose solutions blue when iodine intercalates into the amylose helical turns.[40] Since bulky and charged substituents, like carboxymethyl (CM) groups, may inhibit the formation of helical turns as compared to native amylose (which again was checked with the iodine test[40]), or have an influence on the secondary structure, we speculate that, in solution, secondary structure elements in amylose do not contribute significantly to its elasticity, at least within the resolution of the AFM methodology.

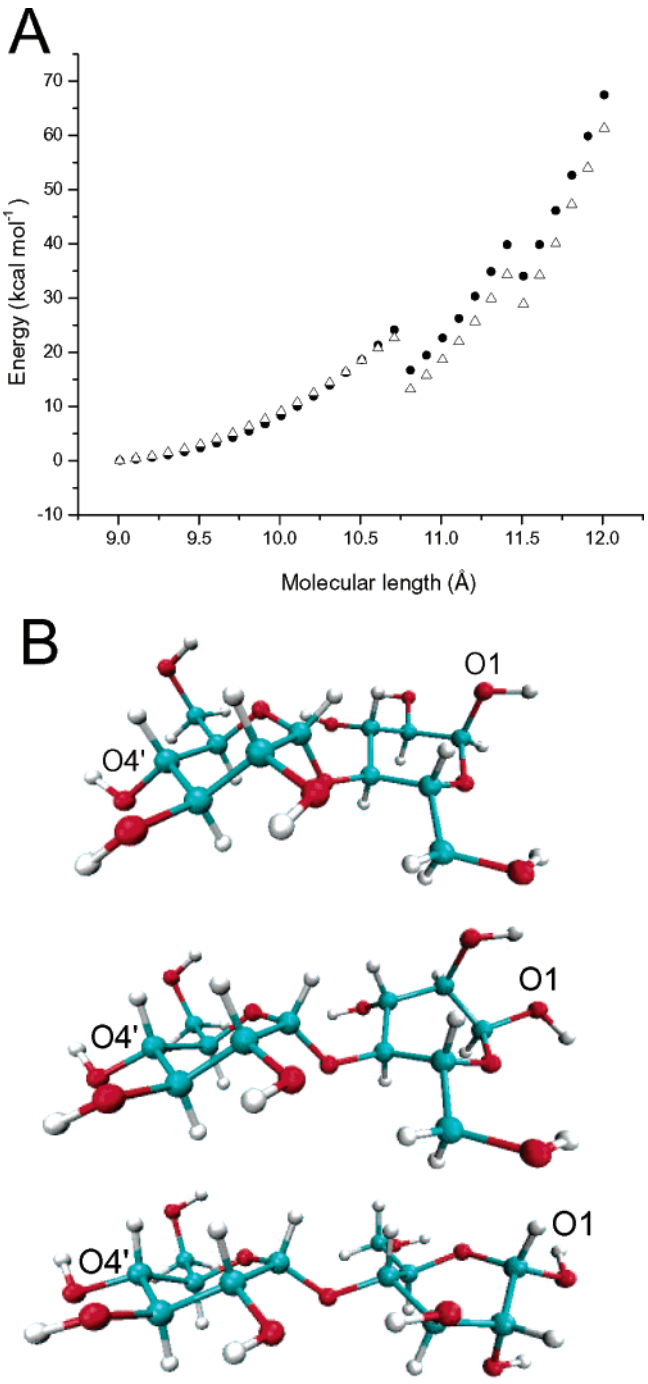

Figure 2. Potential energy surface scan for the O4′−O1 distance of maltose. (A) Energy profiles for stretching the maltose molecule: ●, B3LYP/6-311++G(d,p); △, SCC-DFTB. (B) The structures of maltose at O4′−O1 distances equal to 9.0 (top), 10.8 (middle), and 11.5 Å (bottom).

Mechanical Properties of Maltose. The mechanical properties of a single glucopyranose ring have been previously studied by both molecular mechanics and ab initio calculations.[14,17] Here we present DFT calculations for maltose, which is an α(1→4)-linked dimer of glucopyranose and the shortest amylose

(40) Rao, V. S. R.; Foster, J. F. *Biopolymers* **1965**, *3*, 185−193.
(41) Everett, W. W.; Foster, J. F. *J. Am. Chem. Soc.* **1959**, *81*, 3464−3469.

Table 1. Geometry Parameters Obtained from the Potential Energy Surface Scan for the O4′−O1 Distance of Maltose

distances (Å)			angles (deg)				
O4′–O1	O4′–O4	O4–O1	C1′–O4–C4	O4–C1′–C2′–O2′	O1–C1–C2–O2	O5′–C1′–O4–C4 (Φ)	C1′–O4–C4–C5 (Ψ)
9.0	4.55	4.67	120.3	57.3	56.9	93.9	88.0
9.1	4.57	4.72	120.7	56.7	55.4	93.9	89.2
9.2	4.61	4.78	121.0	56.0	53.8	93.9	90.3
9.3	4.64	4.83	121.2	55.2	52.2	93.8	91.4
9.4	4.68	4.89	121.5	54.4	50.5	93.8	92.4
9.5	4.71	4.94	121.8	53.5	48.6	93.7	93.3
9.6	4.75	5.00	122.0	52.6	46.7	93.7	94.2
9.7	4.79	5.05	122.3	51.6	44.7	93.7	95.2
9.8	4.83	5.11	122.6	50.6	42.6	93.8	96.1
9.9	4.87	5.16	122.8	49.5	40.4	93.9	96.9
10.0	4.91	5.22	123.1	48.3	38.0	94.1	97.5
10.1	4.95	5.27	123.4	47.2	35.4	94.4	98.2
10.2	4.99	5.33	123.7	46.0	32.7	94.7	98.7
10.3	5.04	5.38	124.0	44.7	29.8	95.1	99.2
10.4	5.08	5.43	124.4	43.4	26.4	95.8	99.2
10.5	5.12	5.49	124.7	42.2	22.5	96.6	99.0
10.6	5.16	5.54	125.1	41.0	17.5	97.6	98.4
10.7	5.19	5.61	125.2	40.1	8.9	98.9	96.6
10.8	5.19	5.67	124.5	39.5	−52.5	105.0	92.9
10.9	5.27	5.69	125.5	36.8	−52.6	105.9	95.6
11.0	5.34	5.72	126.6	34.3	−52.7	106.7	97.8
11.1	5.41	5.75	127.6	31.5	−52.8	107.0	100.7
11.2	5.47	5.78	128.7	28.7	−52.9	107.0	103.6
11.3	5.54	5.82	129.8	25.9	−53.0	106.6	107.0
11.4	5.60	5.85	130.9	22.6	−53.0	105.1	112.7
11.5	5.70	5.83	121.8	18.3	−51.3	126.2	−121.3
11.6	5.76	5.87	122.4	16.6	−51.3	126.9	−121.00
11.7	5.81	5.92	123.1	15.0	−51.2	127.3	−120.9
11.8	5.86	5.98	123.8	13.9	−49.9	128.0	−122.2
11.9	5.91	6.02	124.4	12.5	−50.2	128.3	−121.6
12.0	5.96	6.07	125.0	11.3	−50.5	128.6	−121.1

Table 2. Φ and Ψ Values for the Amylose Fragments[a]

amylose fragment	state	angle	1–2	2–3	3–4	4–5	5–6	6–7	7–8	8–9	9–10
antiparallel	initial	Φ	91.8	86.1	86.8	76.4	75.5	84.1	93.6	78.5	77.5
		Ψ	46.3	70.7	61.1	57.3	30.0	63.2	68.0	64.5	80.1
antiparallel	final	Φ	101.4	94.9	125.7	94.4	100.3	121.9	120.6	110.7	120.4
		Ψ	−162.6	−146.6	−132.3	−139.5	−153.2	−119.3	−159.6	−145.5	−134.6
randomized	initial	Φ	90.3	83.0	104.0	95.8	77.3	109.8	106.8	83.1	96.0
		Ψ	−171.8	−153.9	−175.0	158.3	65.0	74.2	75.6	−147.3	−129.6
randomized	final	Φ	110.7	146.0	114.4	92.2	94.9	99.7	74.0	140.6	133.5
		Ψ	−137.7	−125.2	−141.3	−147.3	−165.2	−148.8	−149.2	−142.2	−128.1

[a] The pyranose ring with index 1 has a free hydroxyl group on C4.

polymeric chain. Stretching the maltose molecule involves the conformational changes of the linkage bonds and angles, which are absent in single ring studies.

The ideal approach to study the conformational transitions of molecules is to determine the minimum energy path (MEP) between the initial and final conformations. The structures along the MEP should represent a typical set of transitions. However, this type of calculation is difficult for sugar rings, which have multiple puckering conformations and thousands of orientations for hydroxyl groups. Another approach, the potential energy surface (PES) scan along the O4′−O1 distance, is a simple but useful means to detect the mechanical properties of maltose. The scan covered a wide range of O4′−O1 distances from 9 to 12 Å with a step size of 0.1 Å. The initial optimized structure of maltose has $\Phi = 93.9°$ and $\Psi = 88.0°$, which is a local minimum point according to the previous force field studies.[42,43] (The global minimum point for maltose is around $\Phi = 108°$ and $\Psi = 145°$.[43])

The geometry parameters and energy changes along the scan are shown in Table 1 and Figure 2. The most distinct features of the energy profiles displayed in Figure 2A are the two energy jumps occurring at the O4′−O1 distances equal to 10.8 and 11.5 Å. For illustration, the molecule structures at these two points, as well as at the first point, are shown in Figure 2B. Accompanying the first energy jump is the abrupt change of the O1−C1−C2−O2 torsion angle, an observation which indicates that the second sugar ring (the reducing end) switched from an envelope to a boat conformation (Figure 2B middle). Because there are no other significant changes of geometry parameters at this stage, the lowering of the energy indicates that the boat conformation becomes the more stable form for the second sugar ring. The most significant geometry changes, associated with the second energy jump, involve the C4−O4 bond rotation, reflected by the Ψ angle shown in Table 1. As seen from Figure 2B and Table 1, the first ring (the nonreducing end) did not

(42) Naidoo, K. J.; Kuttel, M. *J. Comput. Chem.* **2001**, *22*, 445−456.

(43) Mendonca, S.; Johnson, G. P.; French, A. D.; Laine, R. A. *J. Phys. Chem. A* **2002**, *106*, 4115−4124.

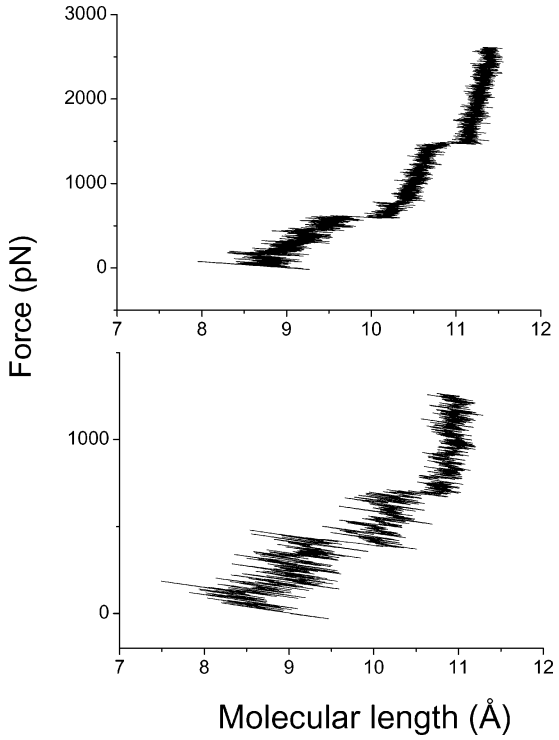

Figure 3. Force−extension curves for maltose in a vacuum (top) and in solution (bottom).

switch to the boat form. Therefore, the lowering of the energy at this point must come from other sources. First, there are dramatic changes for the Φ and Ψ angles. As shown in the energy contour map of maltose but with both rings in the chair conformation,[43] the changes of Φ and Ψ angles may make the greatest contribution to this energy drop. There is also hydrogen bond formation between the O3 and O2′ atoms (Figure 2B bottom, angle O3−H−O2 = 166° and distance O3−O2′ = 3.06 Å) and relaxation of the glycosidic angle (131° changed to 122°).

Our potential energy surface scan demonstrates that the stretching of maltose introduces both deformations of the pyranose rings and changes in the inter-residue geometries. Also, the deformations of the two rings did not happen simultaneously, indicating that the tensions experienced by these two rings seem to be different. However, we note that the constrained optimization may not necessarily reflect the conformational changes of pyranose rings occurring in AFM experiments in which a polymer chain is solvated in water and the entire system is experiencing thermal fluctuations.

The SMD simulation provides an alternative and more direct way to examine the elastic properties of molecules. For electronic structure calculations, we used the SCC-DFTB method, which is computationally feasible for MD simulations. Figure 2A compares the energy profiles of SCC-DFTB and B3LYP calculations. While the two curves agree very well at the low extension region, at the high extension region SCC-

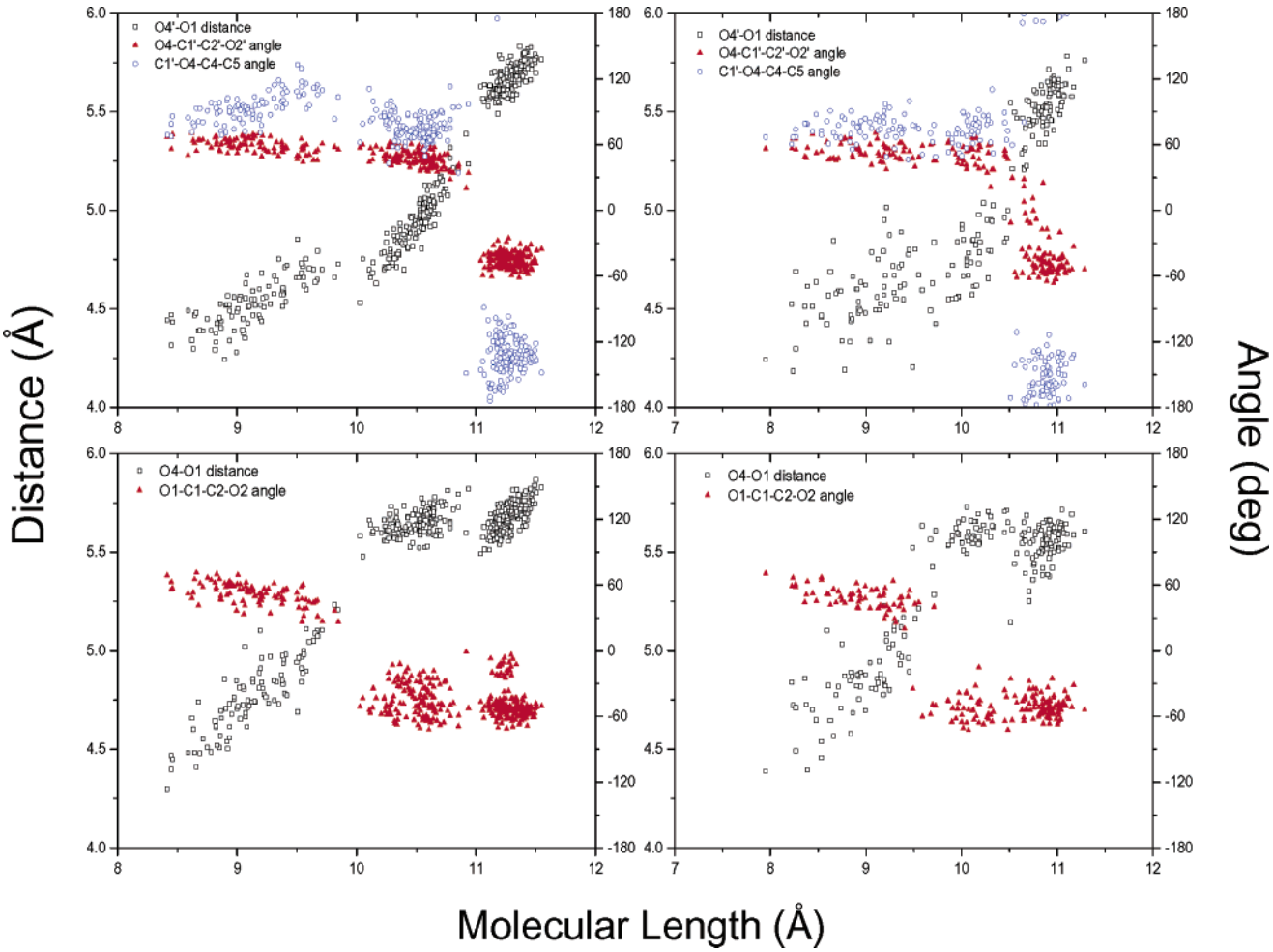

Figure 4. Geometry changes of maltose during the SMD simulations performed in a vacuum (left panels) and in solution (right panels). The geometry parameters of the nonreducing end, as well as the Ψ angle, are shown on the top, and the geometry parameters of the reducing end are shown on the bottom.

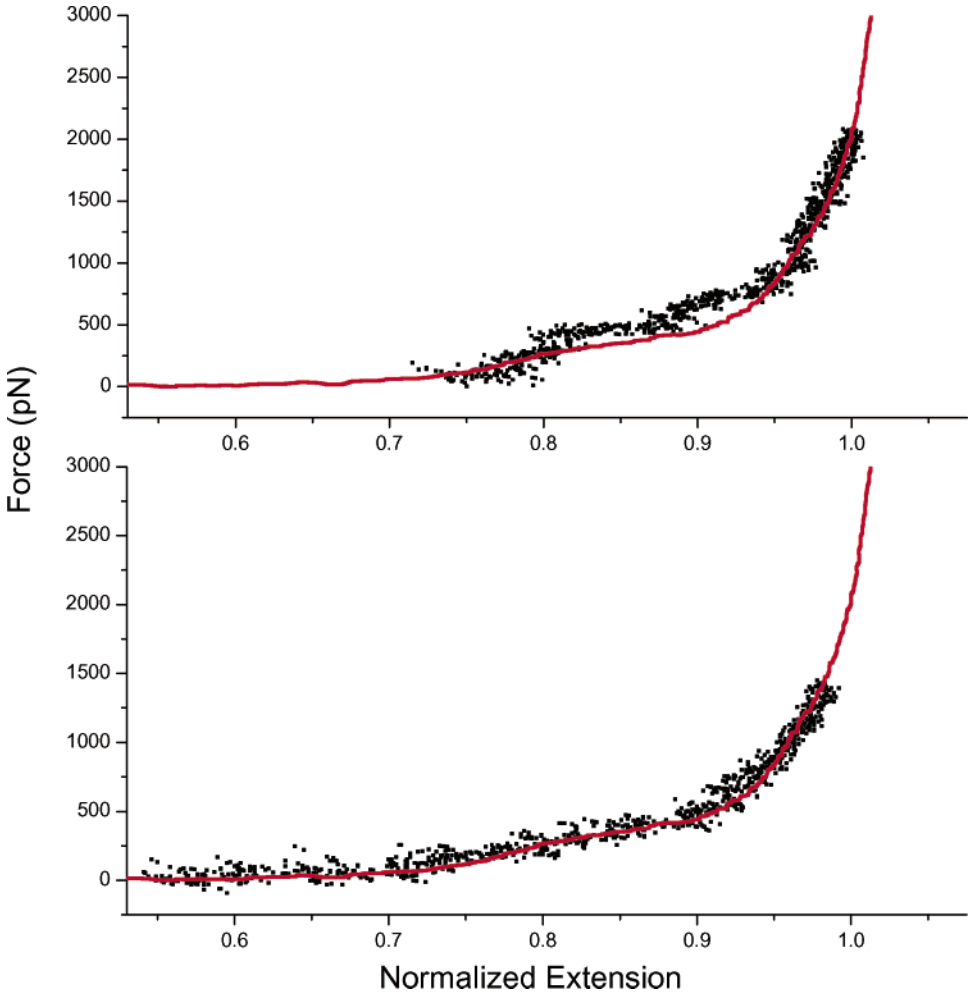

Figure 5. Force−extension curves for the amylose deformation with the antiparallel (top) and randomized (bottom) starting conformations. Red line, experimental force−extension relationship obtained by AFM[3]; black trace, force−extension relationship obtained by QM/MD simulations. The extension was normalized by 55.3 Å, the molecular length determined at a force of 2000 pN.

DFTB tends to underestimate the relative energies as compared with B3LYP. However, the slopes of the two energy curves, which reflect the magnitude of the stretching force, are similar in the entire range of the extension. The biggest difference between the SCC-DFTB and B3LYP energy values is about 6 kcal mol^{-1} at the last point of the energy profile. Compared with the relative energy of 67.5 kcal mol^{-1} given by B3LYP at that point, 6 kcal mol^{-1} error is still tolerable. We consider SCC-DFTB a reliable method for exploring the deformation of amylose.

To investigate the necessity of including the water solvent in the simulations, we performed SMD simulations for maltose both in a vacuum and in solution at a temperature of 300 K. For the starting conformation of maltose, we used the optimized structure from the PES scan with the O4′−O1 distance equal to 9.0 Å. The calculated force−extension curves are shown in Figure 3. Both curves clearly exhibit two plateau features. After inspecting the trajectories saved during the simulations (see Figure 4), we conclude that the first plateau corresponds to the chair-to-boat transition of the second ring, and the second plateau coincides with the C4−O4 bond rotation. Although these phenomena are similar to those observed in the PES scan, there are some differences between these two calculations. Compared with the energy jumps shown in the PES scan, the plateaus in the SMD simulations occurred at lower extensions, and the appearance of the second plateau was also accompanied by the flipping of the first ring to the boat conformation. There are also some differences between the results of the vacuum and solution calculations. In solution, the chair-to-boat transitions occurred at lower forces and smaller extensions. Such differences indicate that the water solvent affects the mechanical properties of maltose. Previous conformational analysis of α-D-glucose[44] and maltose[43] suggests that the solvation "flattens the landscape" and thus reduces the relative energies of the rotamers and local minimum conformations. The direct consequence of a flattened energy landscape is larger conformational fluctuations, which may influence the mechanical properties of glucopyranose rings. The solvation effect observed in our simulations is supported by the results of our most recent AFM experiments, which indicate that the elastic properties of amylose significantly depend on the dielectric constant of the solvent (unpublished).

The description of the conformational changes is given in the Supporting Information. From Figure S1 we see that, after the chair-to-boat transitions, the two sugar rings of maltose are in either a boat or a skew conformation, with the Φ angle varied from 180° to 300°, and the θ angle varied from 80° to 90°.

(44) Cramer, C. J.; Truhlar, D. G. *J. Am. Chem. Soc.* **1993**, *115*, 5745−5753.

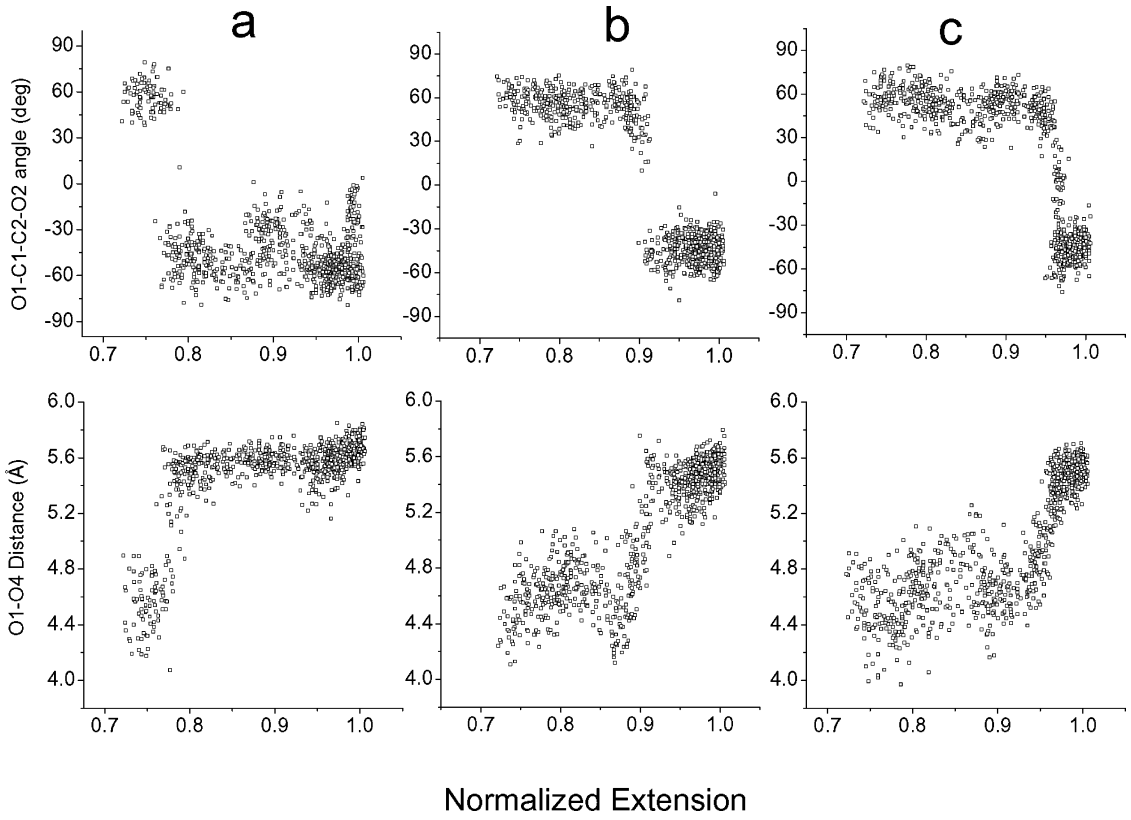

Figure 6. Examples of conformational changes for individual pyranose sugar rings versus the normalized extension of the polysaccharide chain with the antiparallel starting conformation (cf. Figure 5 top). Chair-to-boat transition shortly before, in the middle of, and at the end of the plateau region of the simulated force−extension curve for rings 10 (a), 4 (b), and 2 (c), respectively. Top, O1−C1−C2−O2 dihedral angle; bottom, O4−O1 distance.

Similar distributions of Cremer−Pople pucking-ring parameters are also observed from the simulations of amylose fragments.

Force-Induced Conformational Changes of Amylose Fragments Revealed by SMD Simulations. Because the structure of amylose in solution remains uncertain, we performed two separate SMD simulations with different initial conformations of the amylose chain. One simulation was started with a 2-fold screw axis conformation, as suggested by Heymann and Grubmüller,[18] who termed this conformation "antiparallel configuration". This antiparallel orientation for adjacent glucose residues so far was only found in the crystal structure of cycloamylose,[19] in which 24 of the 26 linkages are still in the common syn orientations. Therefore, this initial two-fold screw axis conformation may not be representative of structures of amylose in solution. Another simulation was started with a conformation having randomized values for Ψ angles. The end-to-end O4−O1 distance after 50 ps of equilibration was 40.3 Å for the antiparallel model and 30.3 Å for the randomized model. The values of Φ and Ψ angles after equilibration are shown in Table 2. Because the single-molecule AFM experiments on CMA contradict the Heymann and Grubmüller's hypothesis that the bulky side groups affect amylose elasticity by restraining the inter-residue rotational flexibility, we decided against using any artificial restraining potential in our QM/MM MD simulations.

Figure 5 compares the force−extension relationships measured by AFM measurements[3] and calculated from our SCC-DFTB/TIP3P MD simulations. It is remarkable that the results of both simulations are in good agreement with the experiment. The simulated force−extension curve of the antiparallel model shows a pronounced plateau similar to the plateau measured by the AFM experiments. The calculated pulling forces corresponding to this region are in a range of 400−800 pN, which is within a factor of 2 of the forces measured experimentally (∼250 pN at the beginning and 400 pN toward the end of the plateau feature). The force−extension curve of the randomized model closely follows the experimental curve, but the plateau feature is less pronounced as compared with the simulation of amylose in the antiparallel model. We note that it is typical for SMD simulations of various AFM stretching measurements to overestimate by orders of magnitude the external forces responsible for various conformational transitions, such as the mechanical unfolding of a protein.[45] The main reason for this discrepancy is that the pulling speeds exercised by SMD are much faster than the extension rates generated in the AFM instrument; therefore, SMD simulations typically proceed far away from equilibrium. In light of this known deficiency, the less than 2-fold difference between the forces calculated from our simulations and measured by AFM is not very significant. To judge with confidence which conformation is closer to the one in solution, simulations with significantly slower pulling speeds and a longer amylose chain are required. However, as we speculated from the AFM experiment on CMA, it is possible that the difference of initial secondary structures may not be reflected in the force−extension relationship.

Our simulations provide the details of the force-induced conformational changes and reveal the mechanism of the stretching process. We clearly observed the force-induced chair-to-boat transitions of the glucose rings. These transitions were detected visually by inspection of the glucose rings, as well as

(45) Lu, H.; Schulten, K. *Proteins: Stuct., Funct. Genet.* **1999**, *35*, 453−463.

mathematically by following the O1−C1−C2−O2 dihedral angles that flipped from about +60° to −60° upon a chair-to-boat transition. The chair-to-boat transition for each individual sugar ring happened abruptly and allowed the O4−O1 distance to be elongated (Figure 6). Five rings in the antiparallel model and six rings in the randomized model made chair-to-boat transitions in the normalized extension range from 0.8 to 0.9, which coincides with the plateau region of the experimental force−extension curve. This observation unequivocally proves that such transitions are responsible for the deviations of amylose elasticity from the freely jointed chain model. The backward transitions from boat to chair were seldom observed from the trajectories of the simulations.

Another process clearly observed from our simulations is related to the mutual orientations of the monomers. With the increased tension in the amylose chain, all the neighboring glucose rings rotated about the C4−O4 bonds to orient themselves in a parallel fashion at the end of the simulations, even though they were initially arranged in an antiparallel orientation (see Table 2). Such a C4−O4 bond rotation was also observed in the force field MD simulations performed by Heymann et al.,[18] but contrary to their conclusion, our results indicate that allowing this rotational flexibility produces the pronounced plateau in the force−extension curve. Although the trajectories show that most of the C4−O4 bond rotations were accompanied by the chair-to-boat transitions, as we observed in the simulations of maltose (see Figure 4), it is still unclear whether this bond rotation is necessary for the transition to happen. If the C4−O4 bond rotation does influence the deformation of glucopyranose rings, then the similarity of the elastic properties of amylose and CMA implies that the bulky substituents do not prevent this inter-residue motion.

Conclusions

We report long time scale quantum mechanics simulations of the stretching process of an amylose chain in water and the results of single-molecule AFM stretching measurements on highly derivatized CM-amylose. Our SCC-DFTB/MM SMD simulations reproduce the elasticity of amylose measured from the AFM experiments and reveal that the mechanism of its lengthening transition involves the force-induced chair-to-boat transitions of the glucose rings. Our calculations for maltose also indicate that water affects the mechanical properties of the glucopyranose rings. The AFM measurements demonstrate that substituents do not significantly affect the amylose elasticity. By combining our experimental and modeling results, we conclude that the elasticity of amylose in water is governed by the mechanics of the pyranose rings themselves and their force-induced conformational transitions. Good agreement with experiment and the reasonable time and costs of the calculations make our approach a versatile tool to model reliably a variety of molecular systems involving carbohydrates.

Acknowledgment. This work was supported by grants from the National Science Foundation (P.E.M.) and the National Institutes of Health (W.Y.).

Supporting Information Available: Tables S1 and S2, showing the Cremer−Pople ring-puckering parameters obtained from potential energy surface scan for maltose, and Figure S1, which plots the Cremer−Pople pucking parameter Φ versus θ using the data collected from the SMD simulations for maltose. This material is available free of charge via the Internet at http://pubs.acs.org.

JA031940X